INL/RPT-23-74423 Rev:000

Interface Problem Formulation Improvements with Application to Nuclear Fuel Performance Analysis

Technical Report

Antonio M. Recuero[1], Dewen Yushu[1], and Daniel Schwen[1]

[1]Idaho National Laboratory, September 2023

INL is a U.S. Department of Energy National Laboratory
operated by Battelle Energy Alliance, LLC

Interface Problem Formulation Improvements with Application to Nuclear Fuel Performance Analysis

Technical Report

Antonio M. Recuero[1], Dewen Yushu[1], and Daniel Schwen[1]

[1]Idaho National Laboratory, September 2023

September 2023

Idaho National Laboratory
Computational Mechanics and Materials Department
Idaho Falls, Idaho 83415

http://www.inl.gov

Prepared for the
U.S. Department of Energy
Office of Nuclear Energy
Under U.S. Department of Energy-Idaho Operations Office
Contract DE-AC07-05ID14517

Page intentionally left blank

ABSTRACT

The U.S. Department of Energy's Nuclear Energy Advanced Modeling and Simulation Program aims to develop predictive capabilities by applying computational methods to the analysis and design of advanced reactor and fuel cycle systems. This program has been providing engineering-scale support for the development of BISON, a high-fidelity and high-resolution fuel performance tool.

This report documents new developments and robustness improvements in mechanical and thermal (gap heat transfer) contact formulations. The improvements range from the migration of industrial level ("assessment") nuclear fuel model setups to the usage of mortar formulations, the addition of frictional contact to one-dimensional layered representations of fuel and cladding components, and the addition of the Petrov-Galerkin approach to dual mortar, which improves performance on curved, relatively coarse meshes. In addition, the Lagrange-multiplier enforcement of mechanical mortar contact constraints has been extended to two additional types of enforcement: penalty and augmented Lagrange-Uzawa. We show that the latter approach yields the same interface results as dual mortar in the Multiphysics Object-Oriented Simulation Environment, with the advantage of not worsening the condition number of the system matrix—thereby enabling the use of some general implementations of iterative preconditioners, at the expense of additional system evaluations (i.e., augmentations).

Acknowledgment

This report was authored by a contractor of the U.S. Government under contract no. DE-AC07-05ID14517. Accordingly, the U.S. Government retains a non-exclusive, royalty-free license to publish or reproduce the published form of this contribution, or allow others to do so, for U.S. Government purposes.

This research made use of the resources of the High Performance Computing Center at Idaho National Laboratory (INL), which is supported by the Office of Nuclear Energy of the U.S. Department of Energy and the Nuclear Science User Facilities under contract no. DE-AC07-05ID14517.

Declaration of Competing Interest

The authors declare that they have no known competing financial interests or personal relationships that could appear to have influenced the work reported in this technical report.

Orcid

Antonio Recuero 0000-0002-2611-1812
Dewen Yushu 0000-0002-9692-3955
Daniel Schwen 0000-0002-8958-4748

Contents

List of Figures

List of Tables

Listings

Acronyms

INL Idaho National Laboratory

1. Introduction

Key aspects of a consistent weak enforcement of interface constraint problems were implemented over the past few years (see Yushu et al. (2021); Recuero and Yushu (2022) for formulation fundamentals, which will not be outlined in this document). These aspects include the generation of the mortar segment mesh, for two- and three-dimensional domains, the implementation of a dual mortar approach to mechanical contact using a primal-dual active set strategy, and the use of mortar enforcement for fuel rod thermal interface problems, including light-water reactors (LWR) gas conductance, radiation, and solid-solid interaction contributions. All these developments have come together to provide a more robust and (virtually) numerical-artifact free solution that we propose as the new interface problem modeling standard for nuclear fuel performance problems in BISON, particularly as it relates to two-dimensional and axisymmetric problems (i.e., problems of moderate size). Along these lines, in this report, we describe the migration of BISON assessment cases to use mortar-based formulations, which improve the interface solution (Recuero et al. (2022)) and enable the consideration of friction on the fuel-cladding interface. A Petrov-Galerkin (PG) approach to the mortar mechanical constraints was also added as part of this work. The use of standard (as opposed to dual) Lagrange functions to interpolate gaps and tangential velocities improve the description of weighted quantities on coarse, curved interfaces (Popp et al. (2013)) and, therefore, lead to better convergence.

Layered approaches to the modeling and simulation of fuel rods have enjoyed popularity in traditional fuel performance codes (Lassmann and Blank (1988)). We have enhanced the mechanical contact description in one-dimensional, layered models (also known as "1.5D") to include Coulomb friction between fuel and cladding layers, allowing for sticking and sliding behavior whose kinematic slip is obtained from the out-of-plane generalized strain at each layer. While this development does not represent an advancement in the state-of-the-art nuclear fuel performance simulations in BISON, it allows for fast-running, more accurate simulations that can be coupled with stochastic methodologies, such Bayesian uncertainty quantification (Dhulipala et al. (2023)), to better predict model parameters and sensitivities.

Finally, as a tangible step towards scalable mortar contact simulations, we have expanded frictionless and Coulomb contact behavior to be enforced via an augmented Lagrange (AL) method with Uzawa loops. The results obtained from initial verification problems attest to the fact that the same interface solution for primal and dual variables is achieved with AL compared to the original Lagrange-multiplier approach. The AL approach has the important advantage of being able to maintain a suitable system matrix's condition number, which makes it palatable to iteratively preconditioned solution algorithms, see for example Burman et al. (2023). In particular, even for

a simple problem, the use of AL, as opposed to Lagrange-multiplier-enforced dual mortar, allows for the use of state-of-the-art iterative preconditioners of elliptical equations, such as the hypre Boomer algebraic multigrid[a].

[a]Note that in this document we do not perform an analysis of the performance of iterative preconditioners for contact problems. The implications of the usage of Lagrange multipliers to enforce contact constraints, whether or not they are condensed out, have been analyzed and treated in, for example, Wiesner (2015).

2. Friction for layered light-water reactor modeling in BISON

This task focused on developing a simulation foundational capability for capturing frictional contact between fuel and cladding when modeling the rod height as a succession of one-dimensional layers of finite thickness. That is, we implemented an algorithm that adds the consideration of friction between fuel and cladding layers at the same height when using the one-dimensional, layered approach (see Lassmann (1978)). While the one-dimensional layered approach requires making assumptions on the problem geometry, it can be computationally advantageous over two- or three-dimensional approaches, thereby facilitating running parameter sweeps for sensitivity and uncertainty quantification studies for many BISON nuclear fuel performance simulation analyses.

2.1 Background

Modeling fuel rods as a number of stacked layers has traditionally been a common approach in simulation within specialized software. The fact that fuel rods have a constant or semiconstant axial profile lends itself well to setting up the computer model as a series of line finite elements or layers. These layers can undergo mechanical, thermal, and irradiation loading as the rod power evolves. Additionally, mechanical interaction within the fuel rod imposes radial and axial actions on the fuel-cladding interface. This interface is composed of layer-to-layer points that restrict overall deformation. Approaches to modeling friction within this layered or "1.5D" simulation approach have been proposed and implemented decades ago see, for example, the work of Lassmann (1978, 1980); Lassmann and Blank (1988). These works employ simple conditions to drive layer-wise frictional behavior by branching out axial behavior between sticking and sliding conditions.

The idea of employing friction in layered one-dimensional simulations is adapted here for application in BISON with generic material models, including thermal and irradiation strains, viscoplasticity, fuel-cladding gap heat transfer, coolant thermomechanical effects, and other physics.

2.2 Code Design

Friction acts on out-of-plane strain variables. In the context of layered one-dimensional BISON simulations, the generalized forces acting out of plane are augmented by the influence of friction. The computation of frictional forces and their addition to the out-of-plane variable residual is car-

ried out by two pairs of user objects. Each pair, composed of a nodal and elemental user object, is defined on the fuel and cladding interface, respectively. In each pair, one nodal user object ("Layered1DContactInterfaceStress") computes the effective Young's modulus at the interface, whereas the other user object ("Layered1DFrictionalForce") computes the frictional force.

An input file excerpt outlining the user objects used for the computation of 1.5D frictional forces is in Listing 1.

Also, the elemental user object needs to be provided to the one-dimensional layered tensor mechanics action (see Listing 2).

The frictional contact implementation is currently only available for serial runs, which, however, does not constitute a substantial limitation due to the small problem size of 1.5D simulations.

Listing 2.1. Input file excerpt for the definition of frictional forces.

```
[UserObjects]
  [1DContactStressOOP_fuel]
    type = Layered1DContactInterfaceStress
    direction = y
    stress_name = stress
    num_layers = 10

    direction_min = 0.00917
    direction_max = 0.11591

    block = fuel
    execute_on = 'LINEAR NONLINEAR'
  []
  [1DContactStressOOP_cladding]
    type = Layered1DContactInterfaceStress
    direction = y
    stress_name = stress
    num_layers = 10

    direction_min = 0.00917
    direction_max = 0.11591

    block = clad
    execute_on = 'LINEAR NONLINEAR'
  []
  [1DFriction_secondary]
    type = Layered1DFrictionalForce
    force_postaux = true
    contact_pressure = contact_pressure
    direction = y
    boundary = pellet_outer_radial_surface
    num_layers = 10
    interface_oop_stress_provider_fuel = 1DContactStressOOP_fuel
    interface_oop_stress_provider_cladding = 1DContactStressOOP_cladding
    is_secondary_side = true
    tangential_pressure = tangential_contact_pressure_aux
    friction_coefficient = 0.2
    thickness = 0.01
    penalty_factor = 1.0e13

    direction_min = 0.00917
    direction_max = 0.11591

    scalar_var_name_base_fuel = scalar_strain_yy_fuel
    scalar_num_variable_fuel = 10
    scalar_var_name_base_cladding = scalar_strain_yy_clad
    scalar_num_variable_cladding = 10

    execute_on = 'LINEAR NONLINEAR'
  []
  [1DFriction_primary]
    type = Layered1DFrictionalForce
    force_postaux = true
    contact_pressure = contact_pressure
    direction = y

    boundary = clad_inside_right
    num_layers = 10

    direction_min = 0.00917
    direction_max = 0.11591

    interface_oop_stress_provider_fuel = 1DContactStressOOP_fuel
    interface_oop_stress_provider_cladding = 1DContactStressOOP_cladding
    is_secondary_side = false
    secondary_side_frictional_user_object = 1DFriction_secondary
    friction_coefficient = 0.2
    thickness = 0.01
    penalty_factor = 1.0e13
    scalar_var_name_base_fuel = scalar_strain_yy_fuel
    scalar_num_variable_fuel = 10
    scalar_var_name_base_cladding = scalar_strain_yy_clad
    scalar_num_variable_cladding = 10

    execute_on = 'LINEAR NONLINEAR'
  []
[]
```

Listing 2.2. Input file excerpt for the addition of frictional forces to the out-of-plane residual.

```
[Modules]
  [TensorMechanics]
    [Layered1DMaster]
      [fuel]
        ...
        layer_friction_user_object = 1DFriction_secondary
      []
      [clad]
        ...
        layer_friction_user_object = 1DFriction_primary
      []
    []
  []
[]
```

2.3 Algorithms

The consideration of frictional forces, described in the previous section from the perspective of a user, is outlined here from an algorithmic approach. The single out-of-plane strain for a layer i, ϵ^i_{yy}, is used to ascertain the frictional state of the fuel-cladding interface. In essence, each fuel-cladding layer interface can be: (1) not in contact, (2) sticking (null local relative motion), or (3) slipping (with relative motion and saturated frictional forces).

The employed algorithmic approach can be summarized as follows. Given the out-of-plane layer stiffness, the previous time step's contact pressure, and the incremental, relative out-of-plane strain, one first checks whether the contact pressure is zero. If it is nonzero, one assumes sticking behavior (i.e., the relative, incremental out-of-plane strain) needs to be constrained to be zero. That is achieved numerically by applying a penalty approach on the out of place strain variable with a sufficiently high penalty factor. If the current relative out-of-plane strain increment times the stiffness is larger than the frictional capacity, sticking is not feasible and a constant frictional force opposing the relative motion between fuel and cladding is applied in a way that overrides the previous assumption. This logic is summarized in Algorithm 1.

The penalty coefficients must be selected such that the sticking constraint is enforced properly. This condition translated mainly into two different practical aspects: (1) it must be high enough so that adding a penalty term to the out-of-plane residual is sufficient to guarantee the constraint $\Delta\epsilon_{\text{interface}} \cong 0$ and (2) the penalty factor is not so large that it would hinder numerical convergence by damaging the system's condition number. In practice, we recommend a C value of 10^{13}–10^{15} for BISON's units and typical layered LWR problems.

Algorithm 1 seeks to find out the correct frictional state at each Newton iteration. Without an algorithm that guarantees local convergence, such as the one employed in two- and three-dimensional approaches (Recuero et al. (2022); Recuero and Lindsay (2023)), the layer's frictional states can oscillate between sticking and slipping, thereby hindering the overall system's numerical convergence. For this reason, the default behavior of this algorithm considers a "fixed" frictional state after three Newton or nonlinear iterations, after which the system converges with those fixed, local frictional states—this behavior is outlined in Algorithm 1 with the "Optional" prefix.

Algorithm 1 Frictional 1.5D contact in BISON (primary and secondary surfaces). Computation of F_{fric}.

Require: Matching fuel-cladding layer interface (excluding cladding's plenum layer) [`scalar_var_id`]
Require: Computing the current relative, incremental axial strain: $\Delta\epsilon_{\text{interface}}$
Require: Having normal contact pressure from previous time step available: $p^{\text{old}}_{\text{normal}}$
Require: Out-of-plane transient layer stiffness: E_{layer}
Require: C is a user-defined penalty factor to enforce sticking constraint
Ensure: $\Delta\epsilon_{\text{interface}} = (\epsilon^{t+1}_{yy,\text{cladding}} - \epsilon^{t}_{yy,\text{cladding}}) - (\epsilon^{t+1}_{yy,\text{fuel}} - \epsilon^{t}_{yy,\text{fuel}})$

sliding_sign $= \Delta\epsilon_{\text{interface}}/|\Delta\epsilon_{\text{interface}}|$

▷ If there was contact, assume initially sticking behavior
if $p^{\text{old}}_{\text{normal}} \geq 0$ **then**
▷ Residual for primary/secondary surface at Gauss point
$F_{\text{fric}}(layer) \leftarrow \pm C \cdot$ coord(layer) $\cdot\Delta\epsilon_{\text{interface}} \cdot$ thickness
Optional: Fix layer state within the time step as *sticking*
end if

▷ Check if sticking force is larger than frictional capacity
if $E_{layer} \cdot \Delta\epsilon_{\text{interface}} \geq \mu p^{\text{old}}_{\text{normal}}$ **then**
▷ Assume sliding force and override its value
$F_{\text{fric}}(layer) \leftarrow \pm$ sliding_sign $\cdot\mu \cdot$ thickness $\cdot\, p^{\text{old}}_{\text{normal}} \cdot$ coord(layer)
Optional: Fix layer state within the time step as *sliding*
end if

2.4 Numerical Results

Typically, in fuel-cladding frictional interaction, the stiffness and geometry features of the rods make it such that the usual friction coefficient values, within 0.25–0.8 (see Ma et al. (2021); Sharma et al. (2009)), cause an overall negligible relative motion between fuel and cladding surfaces once they come into mechanical contact.

We employ here a 10-pellet one-dimensional layered example available in the BISON code repository as "1.5D_rodlet_10pellets". The coefficient of friction is varied from a frictionless zero to one. Very low values already generate sticking behavior in the simulation, which causes the cladding and fuel to elongate in a parallel manner[a]. In fact, to obtain an elongation value that captures a mix of stick and slip behavior, coefficient of friction values must be on the order of 0.04. The influence of the coefficient of friction on the overall elongation can be observed in Figure 2.1.

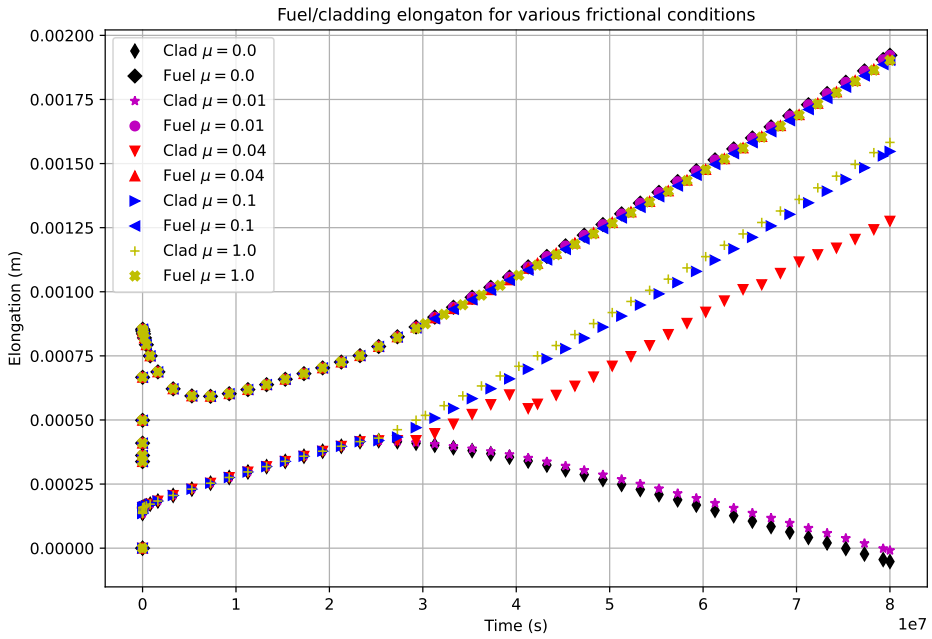

Figure 2.1. Sensitivity of rod elongation with the coefficient of friction. Mechanical contact takes place at about $2.7 \cdot 10^7$ s, when the "softer" cladding component can be mostly driven by the fuel expansion through friction.

Fixing the frictional state of the layers after a number of Newton iterations can have effects on the final mechanical equilibrium of the system. However, this effect is only noticeable when the interaction is close to the Coulomb threshold (i.e., the saturated frictional force). For the case

[a]Note that this result is possible because the top layer of the cladding—the one representing the plenum volume—is excluded from the elongation computation results presented here

presented in Figure 2.2, no difference is observed.

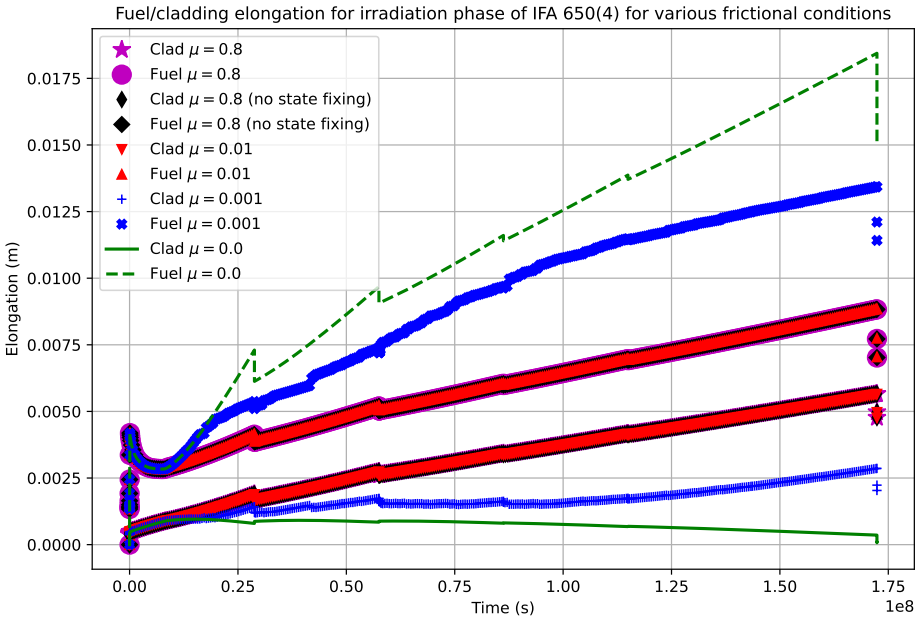

Figure 2.2. Sensitivity of rod elongation with the coefficient of friction for IFA 650. Mechanical contact starts taking place at about $9.0{\cdot}10^6$ s. Very low coefficient of friction values—larger than $\mu = 0.01$—ensure the in-unison axial motion of fuel and cladding. The strategy of fixing the layer frictional interface state does not alter the elongation results (see results for $\mu = 0.8$).

2.5 Comparison Across Dimensions

In this subsection, we compare the fundamental thermomechanical behavior of a fuel rod under variations in the mechanical behavior of the fuel and adhesion conditions of the fuel-cladding interface. This comparison is used as a form of verification of the "1.5D" friction implementation in BISON.

Eleven second-order Lagrange finite elements are used in the radial direction. For the two-dimensional model, 150 finite elements are used for the fuel in the axial direction. Ten layers are used for the layered, one-dimensional setup.

The fuel rod geometry used here has a radius of 4.111 mm, a length of 118.94 mm, an initial gap of 0.0716 mm, an initial plenum height of 25.81 mm, and a cladding thickness of 0.5614 mm.

A convective boundary condition is used to represent the thermomechanical effects of the coolant channel. Its pressure is 15.5 MPa, the inlet temperature is assumed to be 580 K, and mass flux is considered to be constant at 3,800 kg/(m^2·s). The internal rod pressure is accounted for in a plenum pressure model that is a function of moles, temperature, and the volume of the cavity.

Heat transfer and capacities are considered in the model. The thermal conductivity model used for UO_2 is NFIR (see A. Marion (NEI) letter dated June 13, 2006 to H. N. Berkow (US-NRC/NRR) (2006)); the specific heat capacity is computed using the temperature-dependent fit proposed by Luscher et al. (2015). Elasticity of UO_2 is assumed to be isotropic with an elasticity modulus of 200 GPa and a Poisson's ratio of 0.345. The thermal expansion is assumed to be $1.0{\cdot}10^{-5}$ 1/K. A radial relocation model is included in the simulation (see M. A. Kramman (1987)). Fissions per initial heavy-metal atom are computed given the axial power and its axial distribution (see Chapter 10 of Olander (1976)). The isotope fractions for the computation of burnup are 5% and 95% for U235 and U238, respectively. Empirical relations from Allison et al. (1993) are used to compute fuel swelling from both solid and gaseous products; an initial fuel density of 10,431 kg/m^3 is assumed. The inter- and intragranular gas transport of fission products are modeled using the Simple Integrated Fission Gas Release and Swelling (known as Sifgrs, see Pastore et al. (2013)).

The mechanical and thermal models of the Zircaloy-4 cladding are described in what follows. The density is assumed to be 6,551 kg/m^3. The thermal conductivity and the specific heat are selected to be 16 W/(m·K) and 330 J/(kg·K), respectively. Its elasticity modulus and Poisson's ratio are assumed to be 75 GPa and 0.3, respectively. Primary, irradiation, and thermal creep are considered in all numerical results for Zircaloy cladding using Hoppe and Matsuo's models (see Hoppe (1991); Matsuo (1987)). A temperature-dependent thermal expansion model is employed for Zircaloy (see Siefken et al. (2001)). Similarly, strains caused by irradiation are computed according to Franklin (1982).

The heat transfer through the gap and contact fuel-cladding interface is considered using gap conductance, radiation, and solid conduction (if the gap is closed).

The heuristic approach described in Section 2.3 is used to model frictional contact in layered, one-dimensional simulations. A frictional mortar contact formulation that interpolates Lagrange multiplier nodal variables with dual bases is employed for two-dimensional formulations with axisymmetry.

We compare the overall elongation of fuel and cladding components between these two fundamentally different discretization approaches to model the fuel rod axisymmetric problem. In the case of the layered approach, the elongation is computed by accumulating layer-wise axial elongations from each layer's generalized plane strain variable (Cheng et al. (1970)). The elongation of the fuel rod for the two-dimensional model is obtained by capturing the largest axial displacement at the top of the rod.

Both frictional (with a friction coefficient of 0.4) and frictionless results are presented in this section. Three constitutive model options for the fuel range from purely elastic, fuel elasticity and creep, and fuel elasticity, creep and cracking are employed in this work. UO_2 fuel creep is computed using the MATPRO FCREEP material model (see Allison et al. (1993)), including both thermal and irradiation creep. As a third step, cracking effects are included using Barani's fragmentation model (Barani et al. (2019)). The linear heat rate is used as proxy for the number of cracks in the fuel, which is then used to modify (reduce) the elasticity modulus of the fuel material.

Figures 2.3, 2.4, and 2.5 show time-domain elongation results for fuel and cladding for the layered, one-dimensional setup and the traditional two-dimensional axisymmetric approach. Solid lines represent the evolution of the fuel elongation, whereas symbols are employed for the axial

evolution of the Zircaloy cladding. Before the fuel and cladding surfaces come into contact, both fuel and cladding expand under thermal effects. Once the pellet-cladding mechanical interaction takes place at about $3.5{\cdot}10^7$ s, frictional and frictionless axial behaviors diverge. Whereas, for a purely elastic fuel, fuel stiffness is dominant—which is observed in Figure 2.3 in the fuel elongation, as its behavior is hardly affected regardless of whether the fuel-cladding interface is frictional. On the other hand, the cladding elongation closely follows the axial evolution of the fuel if friction is present (see the yellow and blue symbols in Figure 2.3).

As creep and cracking are added to the fuel mechanical behavior (see Figure 2.4 and Figure 2.5), the axial stiffness of fuel and cladding materials become comparable, which results in reduced axial deformation in the fuel. In the three cases, the layered, one-dimensional axial elongation results are in line with those obtained with the variationally consistent dual mortar approach in the two-dimensional axisymmetric model. This exercise serves as one form of verification of the one-dimensional, frictional implementation.

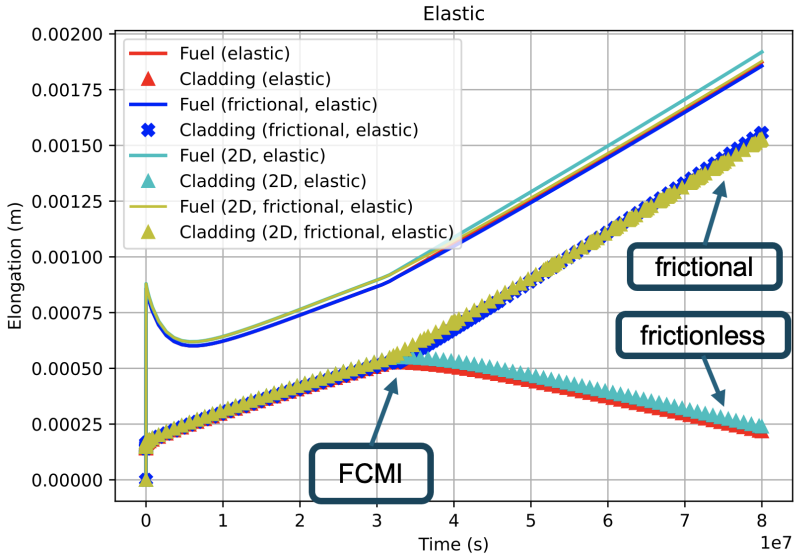

Figure 2.3. Elongation results for elastic fuel. Overall elongation results of both fuel and rod are presented for frictional and frictionless fuel-cladding interfaces. Both axisymmetric and layered, one-dimensional results are presented.

The speedup obtained by the stacked one-dimensional problems over the axisymmetric two-dimensional problem is about 20 times faster on average (135 s for 1.5D and 2,600 s for the two-dimensional axisymmetric problem).

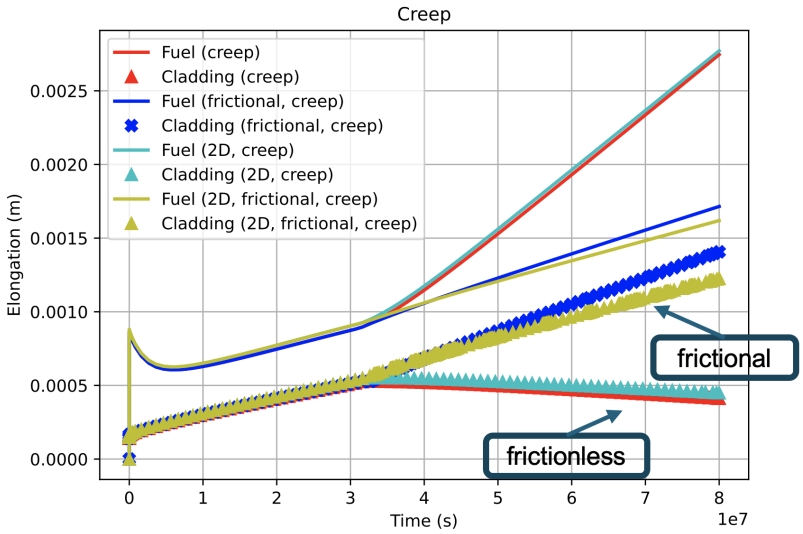

Figure 2.4. Elongation results for fuel with creep. Overall elongation results of both fuel and rod are presented for frictional and frictionless fuel-cladding interfaces. Both axisymmetric and layered, one-dimensional results are presented.

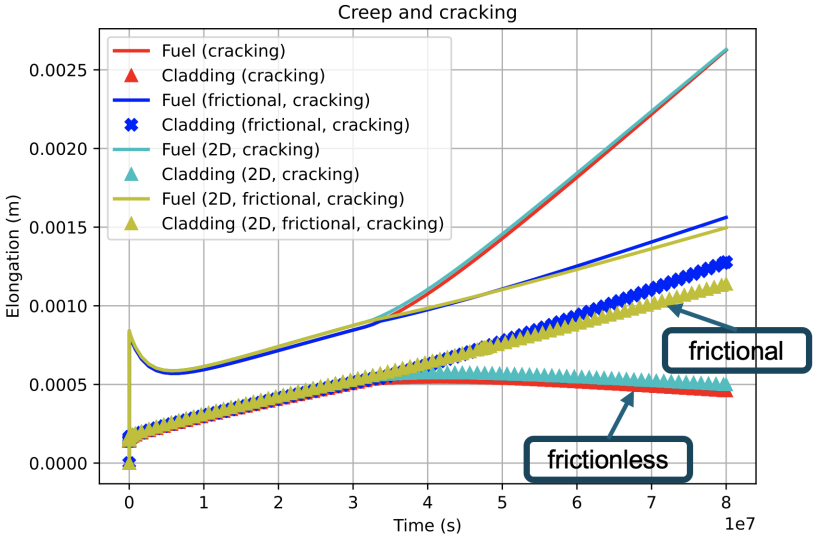

Figure 2.5. Elongation results for fuel with creep and fragmentation. Overall elongation results of both fuel and rod are presented for frictional and frictionless fuel-cladding interfaces. Both axisymmetric and layered, one-dimensional results are presented.

3. Migration of BISON Assessment Cases

To extend the benefits of the mortar finite element framework in the Multiphysics Object-Oriented Simulation Environment (MOOSE), we migrated about 40 LWR fuel-cladding thermomechanical assessment cases in BISON to use mortar enforcement for the gas gap heat transfer problem and mortar mechanical contact with Lagrange multiplier enforcement. These models leverage direct solution strategies (i.e., Super LU) to solve the linear system either using a "Newton" or "preconditioned Jacobian-free Newton-Krylov (PJFNK)" solution strategy to the nonlinear system.

3.1 Assessment Migration

The LWR assessment cases that have been migrated are:

- **Reactivity-initiated accident NSRR**: FK1, FK2, FK3, FK4, FK5, FK6, FK7, FK8, FK9
- **Riso AN**: AN1, AN2, AN3, AN4
- **Calvert Cliffs**: BEN013, BGF092, BHJ027, BFL009, BFL031, BFM034, BFM043, BFM070, BFM071, BFM073, BFM156, UFE019, UFE067
- **Super Ramp**: PK11, PK12, PK13, PK14, PK21, PK22, PK23, PK24, PK62, PK63, PK6S.

This section summarizes changes to the input files. The solution strategy used here leverages a reference residual (absolute residual is also recommended) that converges on the primal system variables (i.e., displacement and temperature variables). The Lagrange multipliers are therefore considered to be converged if displacements and temperature are close enough to the solution. Kernels such as "Gravity" are restricted to higher dimensional domains, that is, we exclude mortar lower dimensional domains from the physics generation since these lower dimensional domains exist only to aid in computing mortar integrals to solve interface problems. If users desire to do so, they can include a "GapConductanceMortar" auxiliary kernel to analyze the overall spatial distribution of gap conductance on the fuel-cladding interface. Mechanical contact is added via the contact action using a "Coulomb" model with a coefficient of friction of 0.4. The algorithmic coefficients for the normal and tangential contact problems, c_n and c_t, respectively, are selected on the order of 10^{12} and 10^{24}, respectively. These coefficients are selected according to the mesh size and numerically representative values for the weighted gap and weighted sliding displacements. Scaling the Lagrange multiplier variables can help better condition the system matrix. Values, such

as 10^{-10} and 10^{-16} for the normal and frictional Lagrange multiplier, respectively, tend to provide the best numerical behavior. The "ThermalContactMortar" action is used to solve the gas gap heat transfer problem, including gap conductance, radiation, and conduction contributions. The normal Lagrange multiplier is provided to consider the normal contact pressure in the computation of conduction between fuel and cladding materials. The selected linear search for the solution is "none," which provides best results when mechanical contact is present.

Other BISON models employing node-to-segment-based thermomechanical formulations can be migrated to using the MOOSE/BISON mortar finite element framework by following the steps described above and by referring to existing migrated input files in the BISON code repository.

3.2 Outcome

The migration of these cases provided, on average, a significant performance boost. Improvements in performance are attributed to:

- The solution is obtained in fewer nonlinear iterations. The better convergence behavior is due to the consistency in the formulation of the interface problem enabled by the mortar method.
- The weak integration rules used for the thermomechanical problem are those dictated by the Lagrange finite element used. Previously, for stability reasons, the interface problem required overintegrating the faces or edges.
- The extra effort required to build lower dimensional mortar segment meshes is more than compensated for with the performance gains.
- For typical axisymmetric BISON models, the newly considered frictional effects are efficiently tackled by the available primal-dual active set strategy algorithm.

Overall, the generalized usage of thermomechanical mortar leads to an efficient consideration of friction, heavily improved interfacial solution to the thermomechanical problem, and faster simulations. Some details on timing results from BISON's assessment nightly suite are given in Figure 3.1.

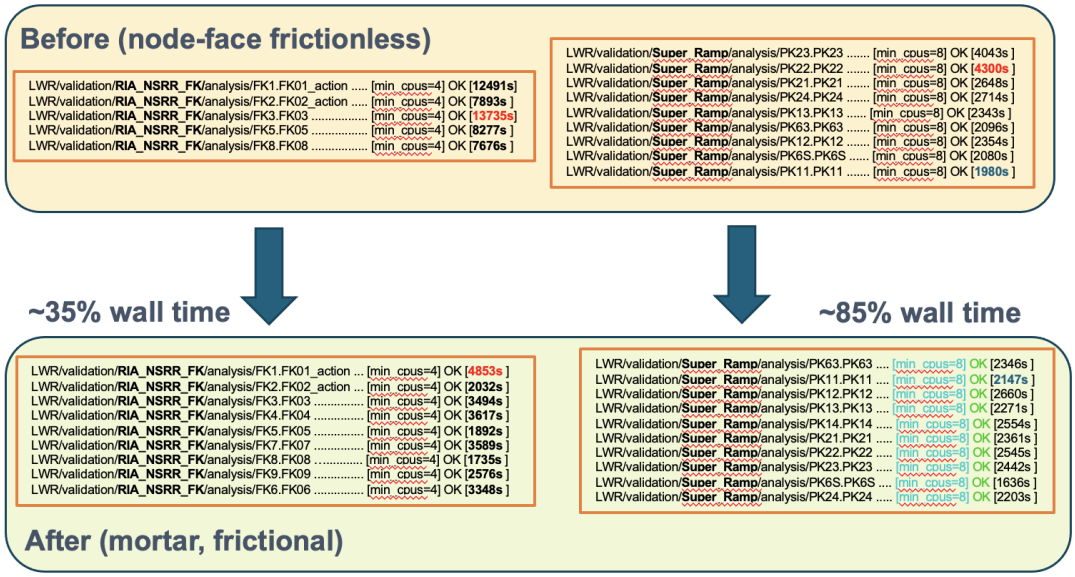

Figure 3.1. Assessment case migration summary. The new cases run in 35%–85% of the time of previous node-to-segment case run-times achieve a superior solution stability on the interface (see Recuero et al. (2022)), avoid discretization artifacts to a large extent, and consider friction on the interface fuel-cladding problem.

4. Petrov-Galerkin Approach

4.1 Background

The Petrov–Galerkin method is a numerical method used to approximate solutions of partial differential equations where the test function and solution function belong to different function spaces. For mortar-based mechanical contact, when the original dual mortar approach is utilized, we may end up with a negative weighted gap value at certain nodes. This negative weighted gap value not only contradicts the continuum setting but may also lead to unacceptable errors or even a nonconverging active set search.

In order to resolve this issue, a Petrov–Galerkin interpolation for the Lagrange multiplier is proposed (e.g., Popp and Wall (2014)). Specifically, dual shape functions are employed for the Lagrange multiplier field, thus resulting in the desired diagonal structure of the mortar matrix, which allows for the condensation of the discrete Lagrange multiplier degrees of freedom (see Yushu et al. (2021)). On the other hand, the interpolation of its variation in the constraint equations is done by standard Lagrange shape functions. To this end, this approach combines the strengths of both standard and dual Lagrange multiplier interpolation methods. Mathematically, this means:

$$\begin{aligned} \lambda &= \sum_{i=0}^{n_\lambda} \Phi_i \lambda_i, \\ \delta\lambda &= \sum_{i=0}^{n_\lambda} N_i \delta\lambda_i, \end{aligned} \tag{4.1}$$

where λ and $\delta\lambda$ are the Lagrange multiplier variable and its variation, respectively, the n_λ is the total number of nodes on the secondary contact interface, the λ_i and $\delta\lambda_i$ are the discretized nodal values of the Lagrange multiplier variable and its variation, respectively, the Φ_i is the dual basis function, and the N_i is the standard basis function.

The PG method is implemented in MOOSE by overwriting the Lagrange multiplier's (dual) test functions using that of a standard Lagrange multiplier variable. This functionality is enabled for all mortar-based constraints, the weighted-gap user object, and the contact action. To use this approach in the contact action, one just needs to set `use_petrov_galerkin=true` in the `Contact` block. To use PG in `Constraints` based input, one needs to enable dual shape function interpolation of the Lagrange multiplier variables (`use_dual = true`). Additionally, one needs to define a

dummy auxiliary variable on the secondary interface that utilizes standard test and shape functions.

4.2 Performance

To demonstrate the performance of the PG implementation, we simulated a hemisphere coming into contact with a round plate (see Figure 4.1(a)). The radius of the hemisphere is 10.87. The round plate has a height of 7.5 and radius of 24.0. The Young's modulus of the hemisphere and the round plate are $1.41{\cdot}10^6$ and $1.0{\cdot}10^5$, respectively. We assume finite strain elastic behavior in both the hemisphere and round plate. The Poisson's ratio of both components are assumed to be 0.0. The dimension and properties of this problem are unit-less for pure demonstration purposes. At the initial stage of the simulation, the hemisphere is tangential to the plate and then pushed down by applying a Dirichlet boundary condition at the top surface. Frictional contact (frictional coefficient 0.3) is simulated by enforcing a mortar-based contact algorithm between the two contact bodies. The hemisphere is pushed down by 0.8 into the round plate at the end of the simulation. We ran the simulation with coarse and refined meshes using HEX8 elements. The coarse mesh has a total of $1,856$ elements, $1,804$ nodes, and $6,783$ degrees of freedom. The fine mesh has a total of $24,320$ elements, $24,282$ nodes, and $78,177$ degrees of freedom. Figure 4.1 shows the problem setting and the normal and tangential Lagrange multiplier variables (contact pressure) at the end of the simulation.

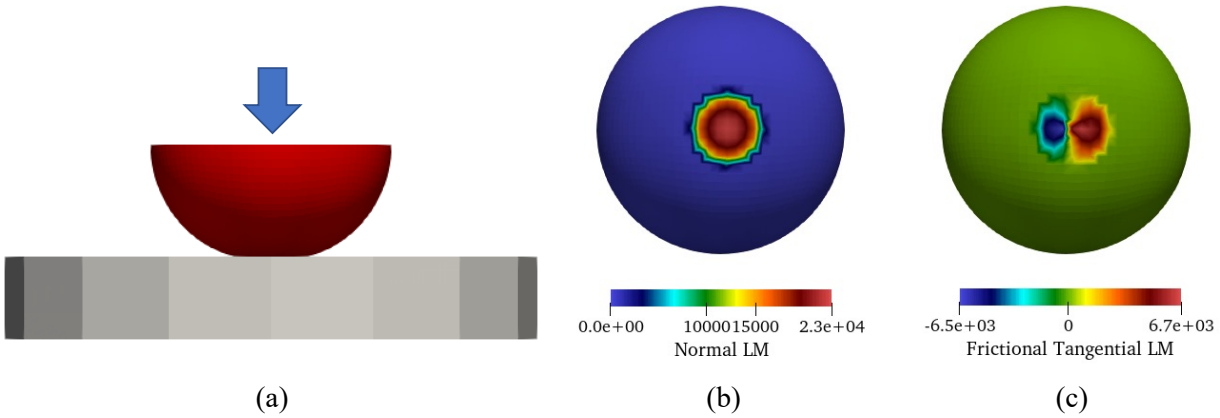

Figure 4.1. Simulation of a hemisphere in frictional contact with a round plate. (a) Problem setup, (b) normal, and (c) tangential Lagrange multiplier fields at the end of the simulation.

Figure 4.2 compares the performance for the above problem between using (blue) and not using (orange) the PG approach. Specifically, Figure 4.2(b) shows that, after using the PG approach, the total number of nonlinear iterations required to solve the problem is reduced for the coarse mesh (by 78 iterations, 13.4% less). The reference approach does not run to completion for the fine mesh, while PG converges the solution using a total of $1,974$ nonlinear iterations. It is worth mentioning that, at the step where the reference approach fails, the PG case already reduces the total nonlinear iteration count by 66. Figure 4.2(c) shows a similar trend for the compute time,

where the PG approach reduces the compute time by 110 seconds (13.27% reduction) compared with the reference approach for the coarse case. For the fine case, the reference approach does not run to completion, while the PG approach converges the solution in $3.15 \cdot 10^4$ seconds.

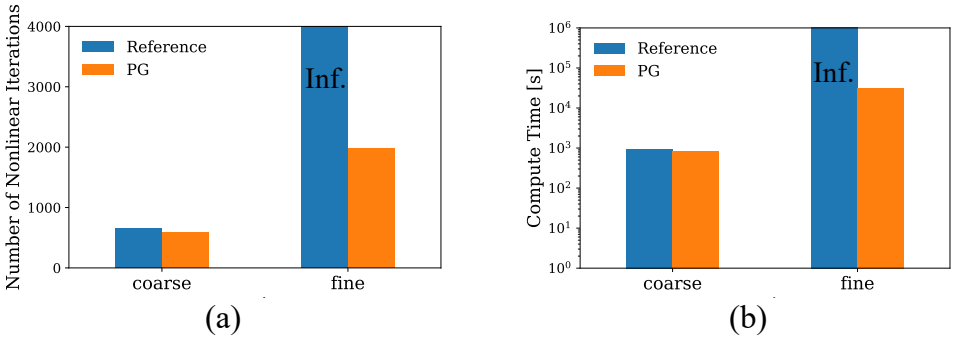

Figure 4.2. Performance improvement brought by PG approach for the half sphere problem (see Figure 4.1) using both coarse and fine meshes. (a) Total number of nonlinear iterations. (b) Total compute time. Note the "Inf." indicates simulation does not run to completion for the typical case.

5. Penalty and Augmented Lagrange Enforcement

5.1 Framework Rework

The MOOSE framework team developed a new user object-based design for the computation of nodal weighted quantities (e.g., weighted normal gaps). The flexible design allows for the Lagrange multiplier, penalty, and AL enforcement of mechanical contact constraints to take place using the same mortar objects.

We migrated contact actions and input files to the new user object-based system and verified that the same results were obtained for all existing regression and verification tests in the MOOSE and BISON repository.

5.2 Penalty Approach

Penalty approaches to constraint enforcement are well known in the optimization and contact mechanics literature. These approaches use a penalty factor to generate an action on the primal variables to reduce the constraint violation.

In the context of a mortar mechanical contact formulation, we have two sets of quantities obtained from the primal variables we work with. First, we calculate weighted gaps, which are used to enforce the normal contact constraints (Wohlmuth (2011); Gitterle et al. (2010); Recuero et al. (2022)). Second, we use weighted slip distances to compute frictional traction on the contacting surfaces.

Weighted gap and relative velocity for two- or three-dimensional problems are computed as usual in MOOSE, by weakly computing gaps and relative velocities on the mortar segment mesh, see eq. (5.1). Note that, unlike the original enforcement we used with Lagrange multipliers, these quantities are interpolated with Lagrange interpolation functions, N_j instead of dual bases ψ_j (this idea is analogous to the PG approach presented in Section 4.1):

$$\begin{aligned} \left(\tilde{g}_n\right)_j &= \int_{\Gamma_c^{(1)}} N_j \mathrm{g}_n^h(\boldsymbol{\xi}) \, \mathrm{d}s, \\ \left(\tilde{\boldsymbol{v}}_{\tau,\mathrm{rel}}\right)_j &= \int_{\Gamma_c^{(1)}} N_j \mathbf{v}_{\tau,\mathrm{rel}}^h(\boldsymbol{\xi}) \, \mathrm{d}s, \end{aligned} \tag{5.1}$$

where the superscript h refers to the discretized evaluation of the quantity and $\boldsymbol{\xi}$ refers to the finite element parametric coordinate. The incremental slip distance is initially computed as $\tilde{\boldsymbol{s}}_{\tau,\text{rel}} = \tilde{\boldsymbol{v}}_{\tau,\text{rel}}\Delta t$, in which Δt is the time step size in an implicit Euler scheme.

Normal and tangential tractions are computed by scaling the weighted gap and slip distances via penalty factors. In essence, the normal pressure and tangential tractions can be obtained as:

$$\begin{aligned} \left(p_n\right)_j &= d_n \left(\tilde{g}_n\right)_j , \text{ and} \\ \left(\boldsymbol{p_\tau}\right)_j &= d_{\boldsymbol{\tau}} \left(\tilde{\boldsymbol{s}}_{\tau,\text{rel}}\right)_j . \end{aligned} \tag{5.2}$$

The quantity $\tilde{\boldsymbol{s}}_{\tau,\text{rel}_j}$ can be accumulated over time and be reset to zero when the node comes out of contact. The tangential components of traction are limited to the Coulomb limit, $|| \left(\boldsymbol{p_\tau}\right)_j || \leq \mu \left(p_n\right)_j$, in which μ is the coefficient of friction.

5.3 Augmented Lagrange

A plain penalty approach to the enforcement of mechanical contact constraints entails a number of limitations that typically render it unusable for industrial applications. Relatively low penalty factors[a] lead to large interpenetration values that tend to underpredict deformation (and typically stress values); high penalty factor values often generate system matrix condition numbers that prevent the adequate solution of the system of equations. This aspect becomes especially sensitive when iterative schemes are used for the computation of the preconditioner matrix (see chapter 6).

5.3.1 Equations and Algorithm

We employ an AL approach via an Uzawa algorithm for iteratively updating contact tractions once the system of equations converges to user-prescribed tolerances (see Simo and Laursen (1992)). This idea gives rise to a loop external to the typical Newton iterations for updating the contact tractions. The outer loop stops once AL iterations reach acceptable values for the fulfillment of the contact constraints. In essence, the interpenetration and slip values for sticking nodes need to be such that the constraints are considered to be correctly enforced. Further, the AL approach can achieve the accuracy of the Lagrange multiplier-based contact enforcement at the expense of additional outer loops in the solution algorithm.

An algorithm describing the implementation in MOOSE Lindsay et al. (2022), partly based on that provided in Wriggers and Laursen (2006), is provided in 2.

Note that the AL enforcement computes nodal contact tractions (i.e., AL multipliers) in an accumulated manner—as opposed to the penalty equations in eq. (5.2). Additionally, $\tilde{g}_n$ and $\tilde{\boldsymbol{s}}_{\tau,\text{rel}}$ are not employed in Algorithm 2 as such, but they are normalized by the mortar segment domain size. As a consequence, the user can choose physical values for the normal gap and tangential slip tolerance values.

[a] Penalty factors need to be compared to the problem physics. In our case, whether the penalty factor is low or high depends on the penalty factor value itself, material stiffness, and mortar segment volumes (domain size).

Algorithm 2 Frictional AL implementation of mortar mechanical contact in MOOSE.

Require: Available displacement vectors $\boldsymbol{u} = \{\boldsymbol{u_x}, \boldsymbol{u_y}, \boldsymbol{u_z}\}$, **internal** Lagrange multiplier variables $\boldsymbol{\lambda} = \mathbf{0} = \{\boldsymbol{\lambda_n}, \boldsymbol{\lambda_{t1}}, \boldsymbol{\lambda_{t2}}\}$, and general penalty factors $\boldsymbol{\epsilon} = \{\epsilon_n, \epsilon_t\}$.
Require: Available AL tolerances TOL_N and TOL_S

while $\texttt{GAP}_{MAX}$ `>` $\texttt{TOL}_N$ `or` $\texttt{SLIPFORSTICKNODE}_{MAX}$ `>` $\texttt{TOL}_S$ **do**

▷ Start solution of multiphysics problem normally.
while $\texttt{USER}_{TOLERANCE}$ `>` Δ $\boldsymbol{u}_{ERROR}$ **do**
▷ Solve system of equations via Newton or Preconditioned Jacobian-free Newton Krylov
$\boldsymbol{Res}(\boldsymbol{u}, \boldsymbol{\lambda}) = \mathbf{0}$
end while

▷ Next step: Check convergence of the AL problem.

▷ Update AL contact tractions for future Newton iterations.
for `All interface nodes` $i = 1...N_c$ **do**
Update $\boldsymbol{\lambda_{n_i}}$ according to increment eq. (5.2).1.
Update $\boldsymbol{\lambda_{t1_i}}$, $\boldsymbol{\lambda_{t2_i}}$ according to increment eq. (5.2).2 and apply Coulomb limit.
Update $\boldsymbol{\epsilon} = \{\epsilon_n, \epsilon_t\}$ with heuristics based on the evolution of the local normal gap and local frictional forces.
end for

end while

5.3.2 Code Design

The penalty AL implementation is based off the `UserObject`-based design for the parallel-consistent computation of weighted normal gaps and weighted tangential velocities (Lindsay et al. (2023)). We extended the AL interface for regular and reference residual problems within the `AugmentedLagrange` scheme. These methods are summarized as:

- `::isAugmentedLagrangianConverged`. This method checks whether the normal gap is less than the user-prescribed gap tolerance and, for the frictional case, whether the slip distance is less than the tangential slip tolerance for nodes that stick (i.e., $\mu\lambda_{n_i} > \lambda_{t_{(1,2)i}}$).
- `::updateAugmentedLagrangianMultipliers`. This step updates the AL multipliers. The nodal $\boldsymbol{\lambda}$ are updated with current, converged weighted normal gaps and weighted tangential slip distances. These values are used as a nodal reference value as the contact tractions are updated using eq. (5.2) in an accumulated manner. This method also outputs the least converged node for normal and frictional contact. In addition, the penalty factor values, ϵ, can be updated at this step to speed up the convergence behavior of the Uzawa algorithm.
- `::(self)initialize` and `::(self)finalize`. These methods are employed to clear and update the contact tractions, respectively, within the Newton iteration schemes.

5.3.3 Examples

Here, we present an initial verification example in two dimensions and assess the numerical results and convergence rate.

The model we use is a plane strain problem with an elastic cylinder pressed on a plane with Dirichlet boundary conditions on the cylinder's mid-plane. Table 5.3.3 provides the parameters used in this model. A visual representation of the numerical results with friction is shown in Figure 5.1.

We compare normal and tangential traction results between the existing Lagrange multiplier-based enforcement (dual mortar) and the newly developed AL algorithm. The normal gap tolerance is selected to be 10^{-7} m when AL is employed. This tolerance value is comparable to the numerical results typically used when the Lagrange multiplier formulation is employed.

Cylinder on Plane	
Parameter	Value
E_{cylinder}	10^6 Pa
E_{plane}	10^{10} Pa
ν_{cylinder}	0.3
ν_{plane}	0.0
Cylinder radius	3.0 m
Y-displacement of mid-plane	0.006 m
Coefficient of friction	0.4
Initial normal penalty	10^6 N/m
Initial frictional penalty	10^7 N/m

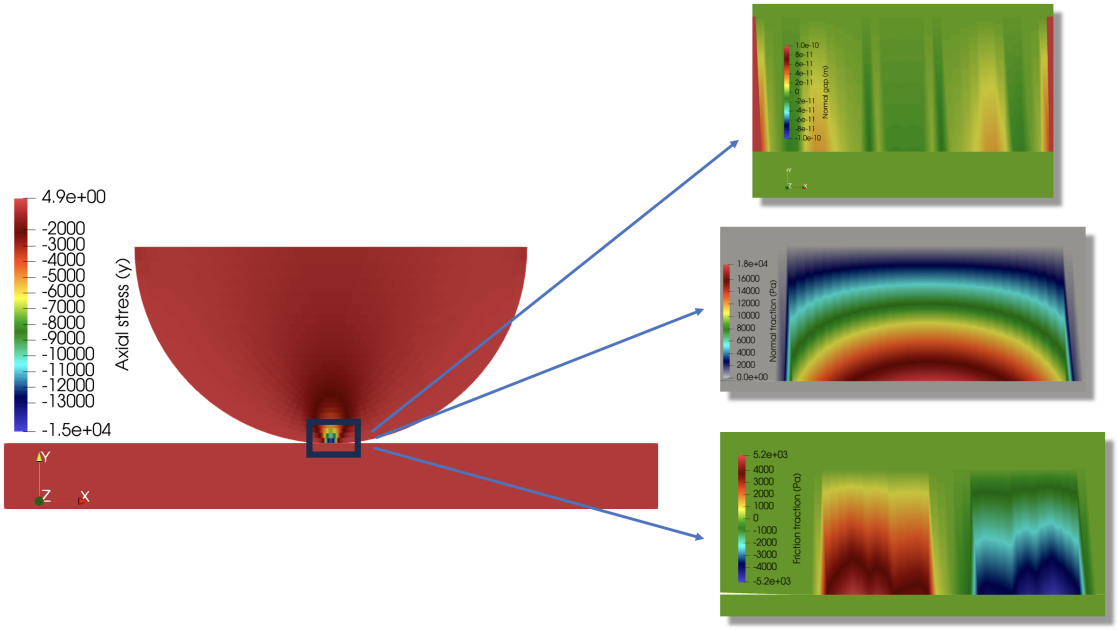

Figure 5.1. Numerical results of a cylinder pressed onto a plane with friction.

Figure 5.2 shows that, provided that an appropriate AL tolerance is input by the user, the normal contact pressure results are equivalent between the two enforcement formulations. It may be of interest to point out that stability and unique solvability requirements (see Wohlmuth (2000); Burman et al. (2023)) apply to the AL enforcement. For this reason, we employ by default dual basis functions for the interpolation of contact tractions (i.e., the implicit-in-the-system Lagrange multipliers). A comparison between using Lagrange interpolation functions and dual bases can be observed in Figure 5.3. The AL method therefore requires analogous care when selecting the interpolation of displacement and Lagrange multiplier variables as the regular Lagrange multiplier enforcement (see Burman et al. (2023) for a recent review on the topic).

The influence of the AL slip distance tolerance on the tangential traction results are shown in fig. 5.4

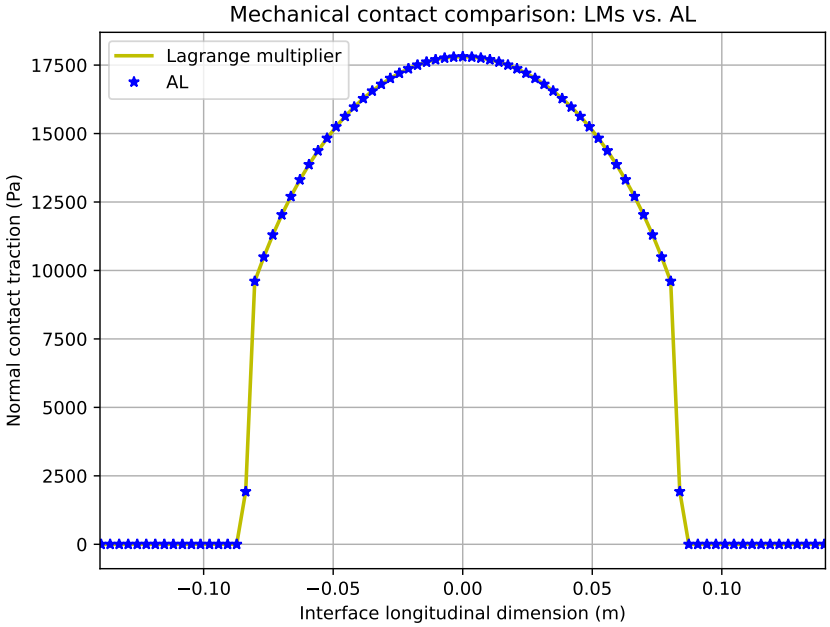

Figure 5.2. Normal pressure obtained from LM and AL.

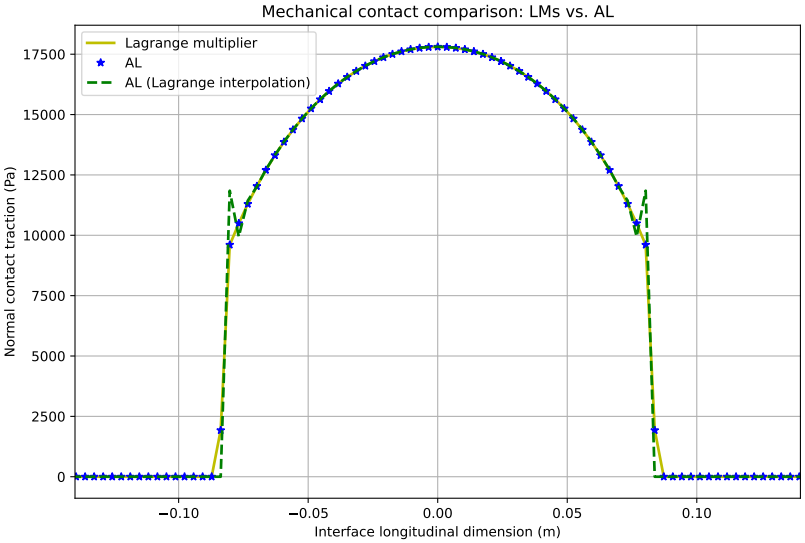

Figure 5.3. Comparison dual basis vs Lagrange interpolations.

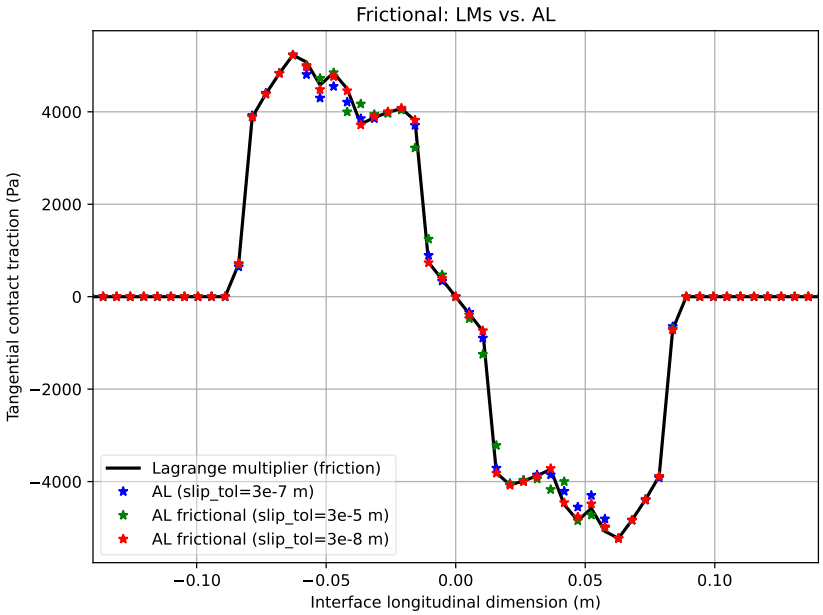

Figure 5.4. Comparison of tangential traction results for various values of slip distance tolerance and the reference primal-dual active set strategy results using dual bases for the Lagrange multiplier variable interpolations.

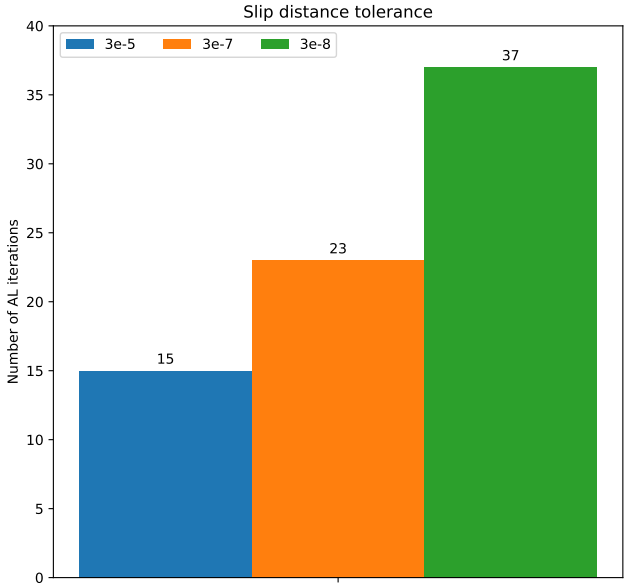

Figure 5.5. Influence of slip distance tolerance on the number of AL iterations. AL iteration adaptivity for the penalty factors was not used.

6. Scalability

The efficient simulation of finite element contact mechanics to simulate large-scale problems poses particular challenges. Iterative preconditioning strategies can aid in solving large-scale contact problems owing to their lower memory footprint. However, the presence of unilateral constraints on the domain boundaries, which are enforced by Lagrange multipliers without further numerical strategies, preclude their use.

Another aspect of mechanical contact is its abrupt, highly nonlinear nature. A large set of nodes can become in contact during the nonlinear (Newton) solves. When this happens, new entries to the system matrix need to be written. For large systems, if these entries had not been allocated, the time spent during allocation can represent the main simulation performance bottleneck.

During Fiscal Year 2023, we identified the latter problem while running three-dimensional reactor core problems with contact. Separately, to alleviate some numerical challenges associated with contact enforcement with system Lagrange multipliers, we implemented the AL method for mortar mechanical contact, whose performance with iterative preconditioners, such as those based on algebraic multigrid (Wiesner et al. (2021)) and additive Schwartz (Adams (2004)), remains to be analyzed and optimized within the MOOSE finite element framework.

6.1 Iterative Preconditioning

This milestone report describes two approaches to facilitate the scalability of mechanical contact problems. Such scalability of contact simulations relies on the successful use of iterative solvers, such as those based on an algebraic multigrid. Using plain penalty approaches to contact results in large system matrix condition numbers that prevent the efficient employment of iterative solvers. In fact, large penalty factors for the enforcement of mechanical contact constraints (as well as others such as penalty Dirichlet boundary conditions), deteriorate the convergence of iterative solvers to the extent that their use is rendered unfeasible. This negative impact of poor system matrix condition numbers can in practice add to the challenges of running finite element models with millions of elements, as the memory requirements of direct solvers can be prohibitive on regular computing desktops and high-performance computing distributed systems.

To alleviate these scalability issues, which are more often encountered in three-dimensional simulations, the mortar mechanical contact framework developed in MOOSE and BISON now offers two solutions (see Brunßen et al. (2007) for extended details):

- Lagrange multiplier enforcement with dual bases and their condensation using the variable

condensation preconditioner. Exact enforcement does not deteriorate, if properly used, the condition number of the global system Jacobian; but it creates additional numerical challenges (Popp et al. (2013)).

- AL approach. At the cost of extra loops to achieve (nearly) exact enforcement of mechanical contact constraints, this method does not deteriorate the system Jacobian condition number and the Lagrange variables never augment the size of the system. Preliminary testing on small contact problems using AL and boomer algebraic multigrid preconditioning has shown good convergence behavior.

6.2 Allocation of New Nonzero Entries

Moderate to large sized problems, the preallocation of matrix memory is crucial to achieving good performance (Balay et al. (2022)). In MOOSE, currently, such allocations take place at the beginning of the simulation or, under some circumstances, at the beginning of the time step. Due to the highly nonlinear nature of mechanical contact, which causes the instantaneous mechanical coupling of degrees of freedom that live on domain boundaries, a large set of variables may be suddenly involved in the solution of the system as the relative normal gap is identified to be less than zero. The identification of contact can often happen during the nonlinear solution process, which, we posit, currently leads to tremendous performance degradation when setting up the system Jacobian. In fact, the few nonlinear iterations in which these allocations occur can take multiple times longer than the rest of simulation for moderate to large problem sizes.

7. Conclusions and Future Work

We have migrated a large set of BISON LWR assessment cases to use the mortar finite element method for interface problems. While such a migration has benefits from both accuracy and performance perspectives, we have also added an AL method to the enforcement of mechanical contact and a PG approach, as an extension to the existing dual mortar approach. Testing and optimization of AL and, to some extent PG, remains to be done in larger and 3D problems. In particular, the local adaptivity of penalty factors (ϵ_t and ϵ_n) for both the normal and frictional problem remains as future work Bussetta et al. (2012). Scalability analyses for the AL method and wider application of the PG approach remain future tasks.

Other proposed, future tasks are:

- **Ensure robustness in the computation of dual basis coefficients**. The Cholesky decomposition of second-order elements (e.g., HEX27) shape functions, used to compute dual basis coefficients, sometimes encounters non-positive definite matrices. This may be caused by numerical error from various sources during contact geometry and solution updates.
- **Provide users with guidance on hard-to-select contact parameters**. Sensitivity studies for performance in the primal-dual active set strategy equations c_n and c_t will be performed. This effort will also aim to provide automatic selection of such coefficients.
- **Ensure the robustness of variable condensation preconditioning in BISON and 3D problems**. We will employ Cartesian Lagrange multipliers and variable condensation preconditioning in three-dimensional problems.
- **Improve the modeling of the TRISO fuel interface problem: Cohesive zone modeling using mortar**. This task will: (1) develop the interface constraint, (2) solve the instability issue inherent to mortar approaches, (3) verify the development in small "regression" problem(s), and (4) make the initial application to TRISO fuel in BISON.
- **Explore the usage of iterative preconditioning in BISON problems**. In particular, we propose enabling the usage of mortar AL mechanical contact and mortar gap heat transfer analysis with iterative preconditioning. Initial testing this fiscal year showed that adding Lagrange multiplier-enforced thermal contact caused an unacceptable performance of mortar-based thermomechanical problems. That issue will be investigated and addressed.

- **Investigate adaptive mesh refinement with contact error estimators**. Allow for more accurate mesh discretizations in the presence of thermal and mechanical contact.

Bibliography

A. Marion (NEI) letter dated June 13, 2006 to H. N. Berkow (USNRC/NRR). Safety Evaluation by the Office of Nuclear Reactor Regulation of Electric Power Research Institute (EPRI) Topical Report TR-1002865, "Topical Report on Reactivity Initiated Accidents: Bases for RIA Fuel rod Failures and Core Coolability Criteria". http://pbadupws.nrc.gov/docs/ML0616/ML061650107.pdf, 2006.

Mark F Adams. Algebraic multigrid methods for constrained linear systems with applications to contact problems in solid mechanics. *Numerical linear algebra with applications*, 11(2-3):141–153, 2004.

C. M. Allison, G. A. Berna, R. Chambers, E. W. Coryell, K. L. Davis, D. L. Hagrman, D. T. Hagrman, N. L. Hampton, J. K. Hohorst, R. E. Mason, M. L. McComas, K. A. McNeil, R. L. Miller, C. S. Olsen, G. A. Reymann, and L. J. Siefken. SCDAP/RELAP5/MOD3.1 code manual, volume IV: MATPRO-A library of materials properties for light-water-reactor accident analysis. Technical Report NUREG/CR-6150, EGG-2720, Idaho National Engineering Laboratory, 1993.

Satish Balay, Shrirang Abhyankar, Steven Benson, Jed Brown, Peter R Brune, Kristopher R Buschelman, Emil Constantinescu, Alp Dener, Jacob Faibussowitsch, William D Gropp, et al. Petsc/tao users manual. Technical report, Argonne National Lab.(ANL), Argonne, IL (United States), 2022.

T. Barani, D. Pizzocri, G. Pastore, L. Luzzi, and J.D. Hales. Isotropic softening model for fuel cracking in BISON. *Nuclear Engineering and Design*, 342:257–263, 2019. ISSN 0029-5493. doi:10.1016/j.nucengdes.2018.12.005.

Stephan Brunßen, Florian Schmid, Michael Schäfer, and Barbara Wohlmuth. A fast and robust iterative solver for nonlinear contact problems using a primal-dual active set strategy and algebraic multigrid. *International Journal for Numerical Methods in Engineering*, 69(3):524–543, 2007.

Erik Burman, Peter Hansbo, and Mats G Larson. The augmented lagrangian method as a framework for stabilised methods in computational mechanics. *Archives of Computational Methods in Engineering*, 30(4):2579–2604, 2023.

Philippe Bussetta, Daniel Marceau, and Jean-Philippe Ponthot. The adapted augmented lagrangian method: a new method for the resolution of the mechanical frictional contact problem. *Computational Mechanics*, 49:259–275, 2012.

AH-D Cheng, JJ Rencis, and Y Abousleiman. Generalized plane strain elasticity problems. *WIT Transactions on Modelling and Simulation*, 10:167–174, 1970.

Som LakshmiNarasimha Dhulipala, Daniel Schwen, Yifeng Che, Ryan Terrence Sweet, Aysenur Toptan, Zachary M Prince, Peter German, and Stephen R Novascone. Massively parallel bayesian model calibration and uncertainty quantification with applications to nuclear fuels and materials. 1(1), 6 2023. doi:10.2172/1991585. URL `https://www.osti.gov/biblio/1991585`.

DG Franklin. Zircaloy-4 cladding deformation during power reactor irradiation. In *Zirconium in the Nuclear Industry*. ASTM International, 1982.

Markus Gitterle, Alexander Popp, Michael W Gee, and Wolfgang A Wall. Finite deformation frictional mortar contact using a semi-smooth newton method with consistent linearization. *International Journal for Numerical Methods in Engineering*, 84(5):543–571, 2010.

N. E. Hoppe. Engineering model for zircaloy creep and growth. In *Proceedings of the ANS-ENS International Topical Meeting on LWR Fuel Performance*, pages 157–172, Avignon, France, April 21-24, 1991.

K. Lassmann. Uranus — a computer programme for the thermal and mechanical analysis of the fuel rods in a nuclear reactor. *Nuclear Engineering and Design*, 45(2):325–342, 1978. ISSN 0029-5493. doi:https://doi.org/10.1016/0029-5493(78)90225-X. URL `https://www.sciencedirect.com/science/article/pii/002954937890225X`.

K. Lassmann. The structure of fuel element codes. *Nuclear Engineering and Design*, 57(1):17–39, 1980. ISSN 0029-5493. doi:https://doi.org/10.1016/0029-5493(80)90221-6. URL `https://www.sciencedirect.com/science/article/pii/0029549380902216`.

K. Lassmann and H. Blank. Modelling of fuel rod behaviour and recent advances of the transuranus code. *Nuclear Engineering and Design*, 106(3):291–313, 1988. ISSN 0029-5493. doi:https://doi.org/10.1016/0029-5493(88)90292-0. URL `https://www.sciencedirect.com/science/article/pii/0029549388902920`.

A. Lindsay et al. NEAMS multiphysics milestone report. Tech. Rep. INL/EXT-23-XXXX, INL, United States, 9 2023.

Alexander D. Lindsay, Derek R. Gaston, Cody J. Permann, Jason M. Miller, David Andrš, Andrew E. Slaughter, Fande Kong, Joshua Hansel, Robert W. Carlsen, Casey Icenhour, Logan Harbour, Guillaume L. Giudicelli, Roy H. Stogner, Peter German, Jacob Badger, Sudipta Biswas, Leora Chapuis, Christopher Green, Jason Hales, Tianchen Hu, Wen Jiang, Yeon Sang Jung, Christopher Matthews, Yinbin Miao, April Novak, John W. Peterson, Zachary M. Prince, Andrea Rovinelli, Sebastian Schunert, Daniel Schwen, Benjamin W. Spencer, Swetha

Veeraraghavan, Antonio Recuero, Dewen Yushu, Yaqi Wang, Andy Wilkins, and Christopher Wong. 2.0 - MOOSE: Enabling massively parallel multiphysics simulation. *SoftwareX*, 20: 101202, 2022. ISSN 2352-7110. doi:https://doi.org/10.1016/j.softx.2022.101202. URL `https://www.sciencedirect.com/science/article/pii/S2352711022001200`.

WJ Luscher, KJ Geelhood, and IE Porter. Material property correlations: Comparisons between FRAPCON-4.0, FRAPTRAN-2.0, and MATPRO. Technical Report PNNL-19417 Rev. 2, Pacific Northwest National Laboratory, 9 2015.

Eds. M. A. Kramman, H. R. Freeburn. Escore–the epri steady-state core reload evaluator code: General description. Technical Report EPRI NP-5100, Electric Power Research Institute, February 1987.

Biao Ma, Bin Luo, Zhuozheng Wang, Chuiyi Meng, and Xiujie He. Friction and wear properties of cral-based coatings for nuclear fuel cladding. *Frontiers in Energy Research*, 9:622708, 2021.

Y. Matsuo. Thermal creep of zircaloy-4 cladding under internal pressure. *Journal of Nuclear Science and Technology*, 24(2):111–119, February 1987.

D. R. Olander. *Fundamental aspects of nuclear reactor fuel elements*. Technical Information Center, Energy Research and Development Administration, 1976.

G. Pastore, L. Luzzi, V. Di Marcello, and P. Van Uffelen. Physics-based modelling of fission gas swelling and release in UO_2 applied to integral fuel rod analysis. *Nuclear Engineering and Design*, 256:75–86, 2013.

Alexander Popp and WA Wall. Dual mortar methods for computational contact mechanics–overview and recent developments. *GAMM-Mitteilungen*, 37(1):66–84, 2014.

Alexander Popp, Alexander Seitz, Michael W. Gee, and Wolfgang A. Wall. Improved robustness and consistency of 3d contact algorithms based on a dual mortar approach. *Computer Methods in Applied Mechanics and Engineering*, 264:67–80, 2013. ISSN 0045-7825. doi:https://doi.org/10.1016/j.cma.2013.05.008. URL `https://www.sciencedirect.com/science/article/pii/S0045782513001254`.

Antonio Recuero and Alexander Lindsay. On Practical Aspects of Variational Consistency in Contact Dynamics. *Journal of Computational and Nonlinear Dynamics*, pages 1–13, 01 2023. ISSN 1555-1415.

Antonio Recuero and Dewen Yushu. Implement and test 3d mortar contact in bison. Technical Report INL/RPT-22-69312, Idaho National Lab.(INL), Idaho Falls, ID (United States), 2022.

Antonio Recuero, Alexander Lindsay, Dewen Yushu, John W. Peterson, and Benjamin Spencer. A mortar thermomechanical contact computational framework for nuclear fuel performance simulation. *Nuclear Engineering and Design*, 394:111808, 2022. ISSN 0029-5493. doi:https://doi.org/10.1016/j.nucengdes.2022.111808. URL `https://www.sciencedirect.com/science/article/pii/S0029549322001625`.

Garima Sharma, P.K. Limaye, and D.T. Jadhav. Sliding wear and friction behaviour of zircaloy-4 in water. *Journal of Nuclear Materials*, 394(2):151–154, 2009. ISSN 0022-3115. doi:https://doi.org/10.1016/j.jnucmat.2009.09.001. URL `https://www.sciencedirect.com/science/article/pii/S0022311509007727`.

LJ Siefken, EW Coryell, EA Harvego, and JK Hohorst. SCDAP/RELAP5/MOD3.3 Code Manual: MATPRO-A Library of Materials Properties for Light-Water-Reactor Accident Analysis. Technical Report NUREG/CR-6150, Vol.4, Rev.2, U.S. Nuclear Regulatory Commission, 2001.

J Ci Simo and TA Laursen. An augmented lagrangian treatment of contact problems involving friction. *Computers & Structures*, 42(1):97–116, 1992.

Tobias Wiesner. *Flexible aggregation-based algebraic multigrid methods for contact and flow problems*. PhD thesis, Technische Universität München, 2015.

Tobias A Wiesner, Matthias Mayr, Alexander Popp, Michael W Gee, and Wolfgang A Wall. Algebraic multigrid methods for saddle point systems arising from mortar contact formulations. *International Journal for Numerical Methods in Engineering*, 122(15):3749–3779, 2021.

Barbara Wohlmuth. Variationally consistent discretization schemes and numerical algorithms for contact problems. *Acta Numerica*, 20:569–734, 2011.

Barbara I Wohlmuth. A mortar finite element method using dual spaces for the lagrange multiplier. *SIAM journal on numerical analysis*, 38(3):989–1012, 2000.

Peter Wriggers and Tod A. Laursen. *Computational contact mechanics*, volume 2. Springer, 2006.

Dewen Yushu, Antonio Martin Recuero, Daniel Schwen, Alexander D Lindsay, and Benjamin W Spencer. M3 milestone: Advanced contact 2021. 1(1), 9 2021. URL `https://www.osti.gov/biblio/1836106`.